Electronic Supplementary Material (ESI) for Lab on a Chip.

Supplementary Information

Label-free inertial-ferrohydrodynamic cell separation with high throughput and resolution

Yang Liu,[a] Wujun Zhao,[a] Rui Cheng,[b] Alicia Puig,[c] Jamie Hodgson,[d] Mary Egan,[d] Christen N. Cooper Pope,[d] Petros G. Nikolinakos,[d] and Leidong Mao*[b]

[a]Department of Chemistry, The University of Georgia, Athens, Georgia, USA

[b]School of Electrical and Computer Engineering, College of Engineering, The University of Georgia, Athens, Georgia, USA.

[c]Department of Microbiology, Texas State University, San Marcos, Texas, USA.

[d]University Cancer & Blood Center, LLC, Athens, GA, 30607

*Email: Leidong Mao (mao@uga.edu)

Table S1. Comparison of throughputs and separation resolutions between existing microfluidic methods and the inertial-FCS method

Type	Methods	Flow rate (μl/min)	Throughput（cells/s）	Purity	Separation Resolution	Biological particles separated	Reference
Inertial microfluidics	Spiral system (Dean drag force)	100	6.17E+03	NA	5 μm (10 and 15 μm)	CTCs	[1]
	Spiral channel	1700	2.17E+03	97%	NA	Lymphocytes	[2]
	Spiral devices	1000 - 2000	1.67E+04	NA	2.7 μm (7.32 and 10 μm)	WBCs & RBCs	[3]
	Vortex	350	1.67E+05	57-94%	4 μm (15 and 19 μm)	CTCs	[4]
	Straight channel with microstructures.	100-150	2.50E+04	92-98%	4.4 μm (5.5 and 9.9 μm)	Blood cells (WBCs, RBCs)	[5]
	Curved channel	30-120	5-16E+04	NA	1.5 μm (0.5 and 2 μm)	Bacteria	[6]
Deterministic lateral displacement	DLD device	0.05	NA	NA	140 nm (51 and 190 nm)	NA	[7]
Accoustofluidics	taSSAW	20	3.33E+02	NA	2.6 μm (7.3 and 9.9 μm)	CTCs	[8]
DEP	TDEP	3.3	NA	NA	1 μm (9 and 10 μm)	Monocyte separation	[9]
Pinched flow fractionation	AsPFF	0.3	10	NA	1 μm (1, 2, 3, and 5 μm)	Erythrocytes	[10]
Filtration	Hydrodynamic filtration	10	100	90%	NA	T cells	[11]
	Step Pattern filtration	0.1	128	90	NA	JM cells	[12]
Inertial-Ferrohydrodynamics	Inertial-FCS	1000 - 1200	1.00E+05	11% (spiked cancer cells) 11.70% and 36.39% (two patient samples) 91.60% (lymphocytes)	1 μm (for particles < 10 μm in diameter) 2 μm (for particles 10 – 30)	Cancer cell line, lymphocytes	This work

Reynolds number calculation in the inertial-FCS device

Channel Reynold's number (R_c):

$$R_c = \frac{\rho v L}{\mu} \quad \text{* MERGEFORMAT (1)}$$

$$L = \frac{2 \times W \times H}{(W + H)} \quad (2)$$

Where ρ is density of the fluid, v is the maximum channel velocity, L is characteristic channel dimension, μ is dynamic viscosity of the fluid, W is the channel width, and H is the channel height.

Particle Reynold's number (R_p):

$$R_p = R_c \times (D / L)^2 \quad \text{* MERGEFORMAT (3)}$$

Where D is the particle diameter.

Table S2. Reynold's number in inertial focusing and separation stages

Stage	R_c	R_p
Inertial focusing stage	63.8	1.3
Ferrohydrodynamic separation stage	31.9	0.4

The sample flow rate was 1000 μL min^{-1} and the sheath flow rate was 500 μL min^{-1}.

Table S3: Difference between mean cell diameters from the cancer cell and WBCs validation experiments.

Cell Type	Flow rate (mL/h)	Diameter difference between cells from different outlets (μm)			
		#1 - #2	#2 - #3	#3 - #4	#4 - #5
H1299 lung cancer cells	72	7.05 ± 3.56	3.36 ± 1.58	1.91 ± 1.60	4.82 ± 1.56
H1299 lung cancer cells	60	9.23 ± 5.07	2.29 ± 2.09	3.19 ± 1.92	1.57 ± 2.06
WBCs	60	4.42 ± 3.13	3.04 ± 2.66	3.23 ± 2.47	0.00 ± 1.48

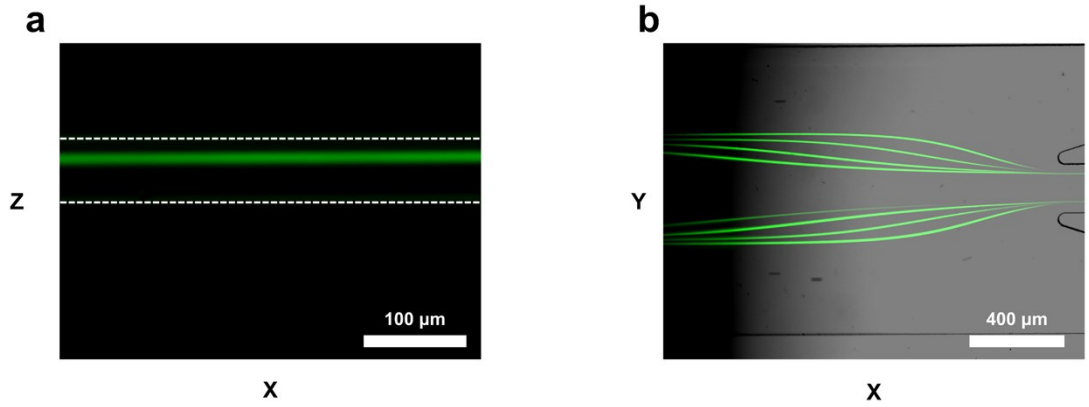

Figure S1. a Side view of inertial focusing of 15 µm polystyrene beads at the sample flow rates of 1000 µL/min in a 0.05% (v/v) ferrofluid in the inertial-FCS device. The ratio of particle flow and sheath flow was 2:1. **b** Top view of inertial focusing of 15 µm polystyrene beads at different sample flow rates (400 -1000 µL/min) in a 0.05% (v/v) ferrofluid in the inertial-FCS device. The flow ratio between sample and sheath flow was 2:1.

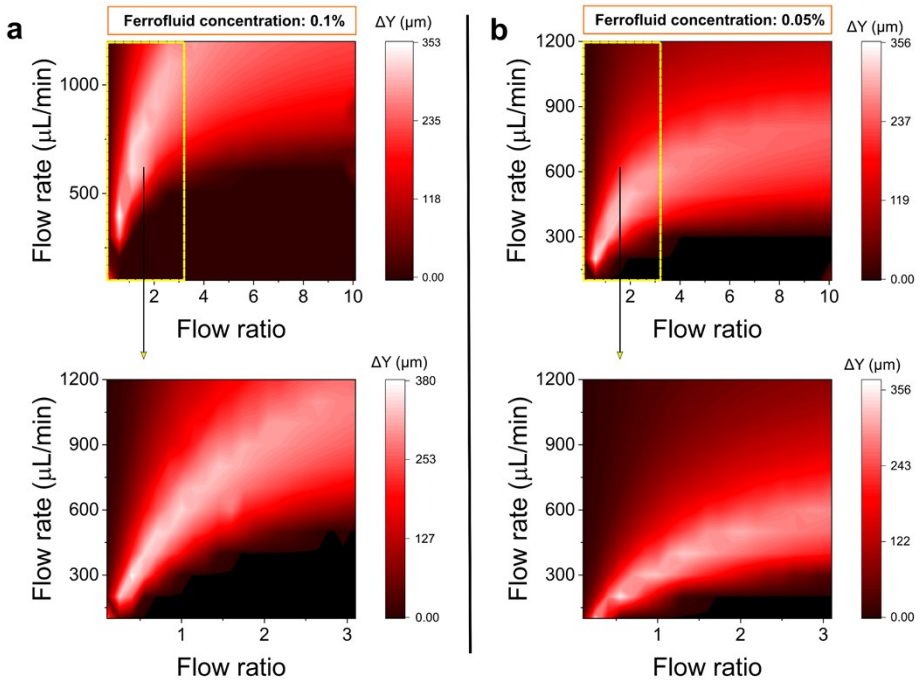

Figure S2. Dependence of diamagnetic particles separation distance (ΔY) on the sample flow rate and the ratio between the sample and sheath flow. **a** Simulation of separation distance between 6 and 10 μm (diameters) diamagnetic particles in 0.1% (v/v) ferrofluid. **b** Simulation of separation distance between 6 and 10 μm (diameter) diamagnetic particles in 0.05% (v/v) ferrofluid.

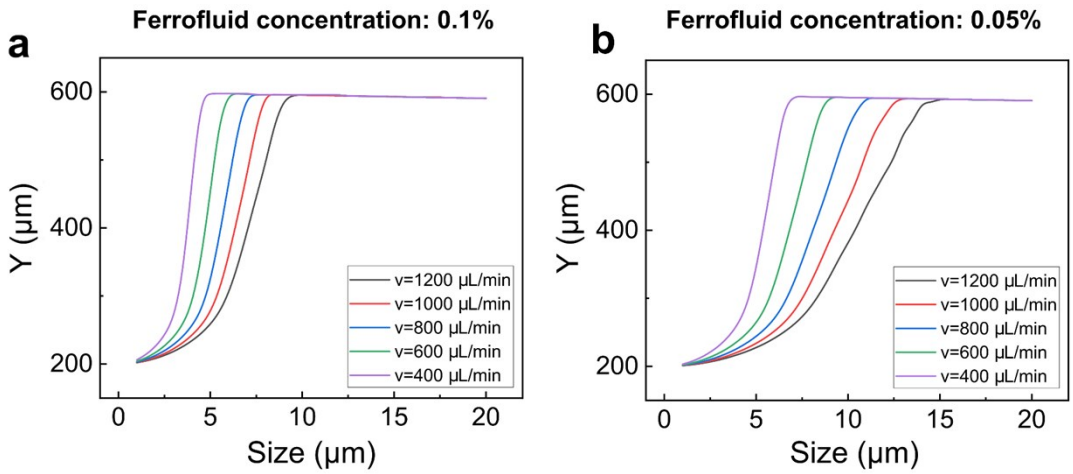

Figure S3. Simulation results of final position of diamagnetic particles of variable diameters, at different sample flow rates (400-1200 μL min-1) in a 0.1% (v/v, **a**) and 0.05% (v/v, **b**) ferrofluid. Simulation results confirmed that the ferrohydrodynamic deflections depended on the particle diameter.

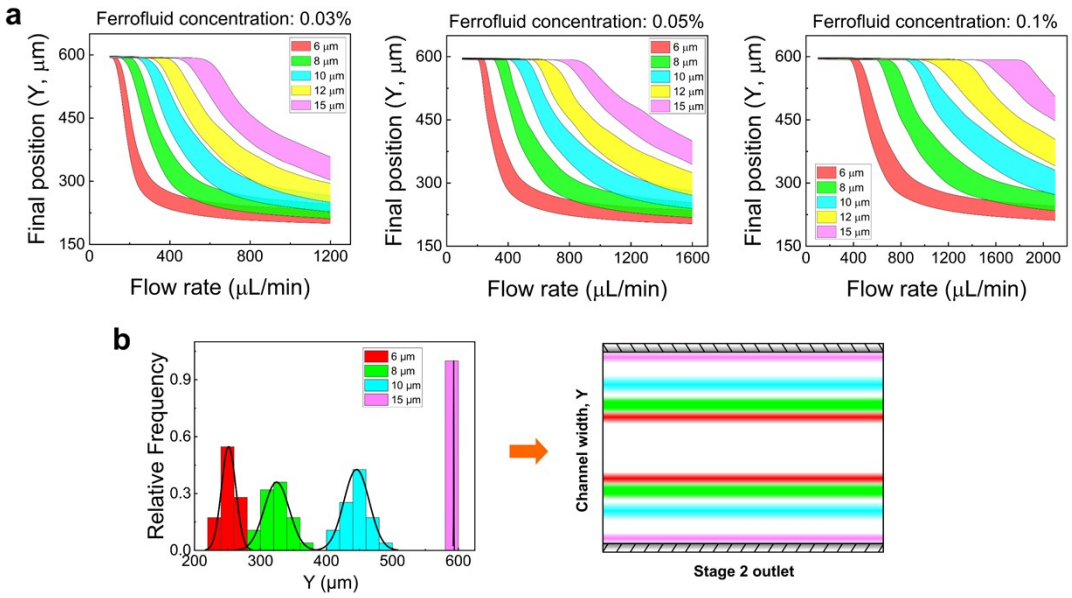

Figure S4. **a** Simulated separation of diamagnetic particles (6 μm, 8 μm, 10 μm, 12 μm, 15 μm diameter) at 100 – 1200 μL/min flow rate in the 0.03%, 0.05% and 0.1% (v/v) ferrofluid. **b** Simulated particles distribution (6 μm, 8 μm, 10 μm, 15 μm) at the outlet of the inertial-FCS device. The ferrofluid concentration was 0.05% and the flow rate was 800 μL/min.

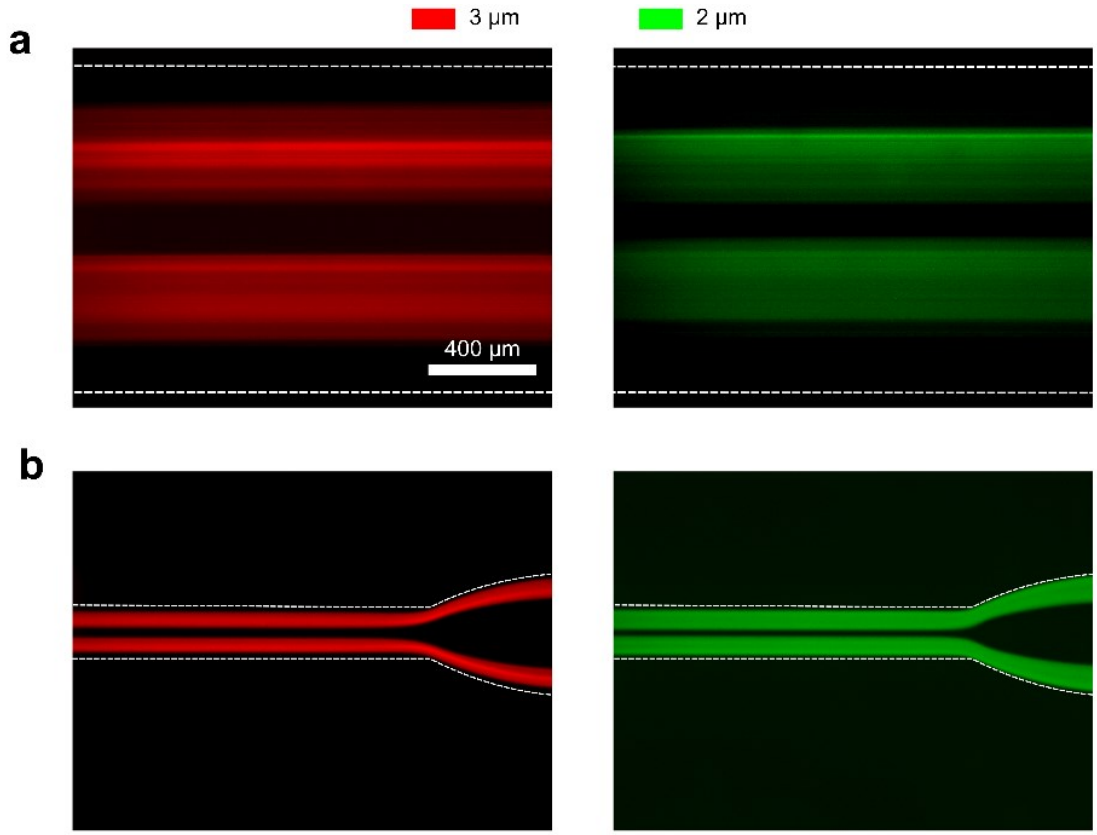

Figure S5. Ineffective inertial focusing of small particles resulted in poor separation. Experimental results of separation of 2 and 3 µm diamagnetic particles in 0.05% ferrofluid at a flow rate of 400 µL/min. **a** Fluorescence images of particle distribution (red: 3 µm, green: 2 µm) near collection outlets showed no spatial separation between the two particles. **b** particle distribution at the end of inertial focusing stage showed ineffective focusing.

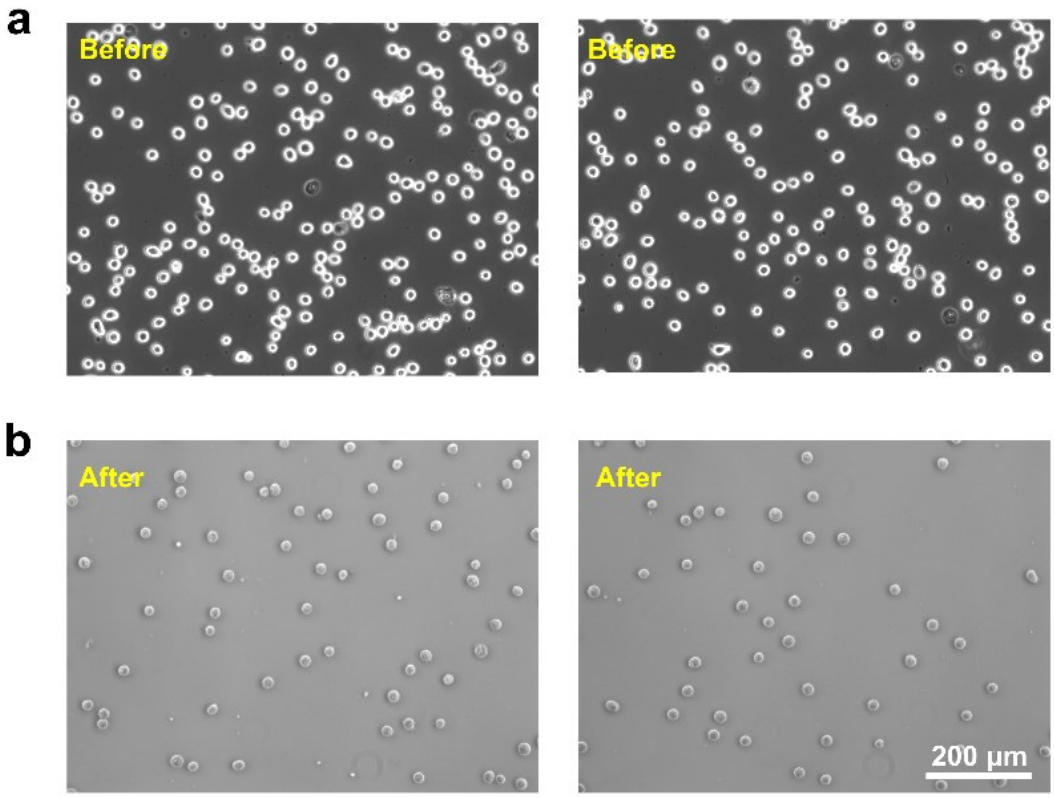

Figure S6. Bright field images of human lung cancer cell line (H1299) before and after the inertial-FCS processing. **a** cells before the inertial-FCS processing. **b** cells after the inertial-FCS processing (flow rate: 60 mL h^{-1}, ferrofluid concentration: 0.05% (v/v)).

Table S4. Morphological comparison of human lung cancer cell line (H1299) before and after the inertial-FCS processing

	Diameter (µm)	Circularity	Aspect ratio	Roundness	Solidity	Number of cells
Before	22.81 ± 4.72	0.88 ± 0.06	1.15 ± 0.20	0.90 ± 0.10	0.96 ± 0.03	500
After	23.54 ± 5.11	0.87±0.07	1.07±0.06	0.93±0.04	0.95 ± 0.01	500

Table S5. CTC isolation purity of patient samples using inertial-FCS

	Cancer type/stage	No. of CTCs per 1 mL of blood	No. of WBCs per 1 mL of blood	Purity (%)
Patient 1	Lung, IV	145	N/A	N/A
Patient 2	Lung, IV	215	N/A	N/A
Patient 3	Lung, IIIB	72	547	11.70
Patient 4	Lung, IIIB	173	302	36.39

Purity is defined as the ratio of the number of CTCs and the number of total cells found at the collection outlet of the inertial-FCS device.

References:

1. M. E. Warkiani, B. L. Khoo, L. Wu, A. K. P. Tay, A. A. S. Bhagat, J. Han and C. T. Lim, *Nature protocols*, 2016, **11**, 134-148.

2. P. L. Chiu, C. H. Chang, Y. L. Lin, P. H. Tsou and B. R. R. Li, *Sci Rep-Uk*, 2019, **9**.

3. N. Nivedita and I. Papautsky, *Biomicrofluidics*, 2013, **7**.

4. E. Sollier, D. E. Go, J. Che, D. R. Gossett, S. O'Byrne, W. M. Weaver, N. Kummer, M. Rettig, J. Goldman, N. Nickols, S. McCloskey, R. P. Kulkarni and D. Di Carlo, *Lab on a Chip*, 2014, **14**, 63-77.

5. Z. Wu, Y. Chen, M. Wang and A. J. Chung, *Lab on a Chip*, 2016, **16**, 532-542.

6. J. Cruz, T. Graells, M. Walldén and K. Hjort, *Lab on a Chip*, 2019, **19**, 1257-1266.

7. K. K. Zeming, N. V. Thakor, Y. Zhang and C.-H. Chen, *Lab on a Chip*, 2016, **16**, 75-85.

8. P. Li, Z. M. Mao, Z. L. Peng, L. L. Zhou, Y. C. Chen, P. H. Huang, C. I. Truica, J. J. Drabick, W. S. El-Deiry, M. Dao, S. Suresh and T. J. Huang, *P Natl Acad Sci USA*, 2015, **112**, 4970-4975.

9. Y.-C. Kung, K. R. Niazi and P.-Y. Chiou, *Lab on a Chip*, 2020.

10. J. Takagi, M. Yamada, M. Yasuda and M. Seki, *Lab on a Chip*, 2005, **5**, 778-784.

11. J. Darabi and C. Guo, *Biomicrofluidics*, 2013, **7**, 054106.

12. M. Mizuno, M. Yamada, R. Mitamura, K. Ike, K. Toyama and M. Seki, *Anal Chem*, 2013, **85**, 7666-7673.